Pool Boiling Heat Transfer Enhancement through Biphilic Stepped Microchannel

AVDHOOT WALUNJ[1*], A. SATHYABHAMA[2]
[1]Dr. A. S. College of Agril. Engineering & Technology, Mahatma Phule Krishi Vidyapeeth, Rahuri-413722, INDIA.
[2]National Institute of Technology Karnataka, Surathkal-575025, INDIA.

Abstract: In present study, pool boiling heat transfer (PBHT) from biphilic stepped microchannel comprising: hydrophobic fin top and hydrophilic channel region is investigated. The biphilic stepped microchannel is prepared by mechanical polishing and thermo-catalytic etching. The improved liquid supply pattern, increased nucleation site density, retarded bubble coalescence between the adjacent channel and decreased wall forces acting on the bubble meniscus resulted in the PBHT enhancement. Contact angle of the water droplet on hydrophobic and hydrophilic surface is 74.02° and 22.5°, respectively. Enhancement in critical heat flux and heat transfer coefficient by the biphilic stepped microchannel is 195.52% and 367.00%, respectively.

Keyword: hydrophobic, hydrophilic, thermo-catalytic etching, bubble coalescence, contact angle

Received: May 26, 2022. Revised: May 7, 2023. Accepted: June 13, 2023. Published: July 12, 2023.

1. Introduction

Mechanism of heat transfer plays a vital role in the numerous industrial and domestic appliances. Electronics devices, condensers, evaporator, HVAC, nuclear power plant, heat exchangers are embedded with relevant heat transfer phenomenon [1]. Nowadays, compact and highly-dense electronic components are adopted worldwide. The thermal stress due to overheating is the serious concern of these miniaturized system components [2]. The generated heat, as a by-product, within the system must be rejected to the surrounding to maintain the system at recommended temperature for its efficient working and prolonged life. The conventional single phase bulky air-cooled system does not withstand the high heat load condition. Passive cooling by pool boiling is cheap, sophisticated and most sustainable embedded cooling system [3]. It has potential to remove large amount of heat. Passive operation of this kind also reduces the overall energy consumption of the equipment. The improvement in the pool boiling heat transfer can be achieved by surface modification like surface coating [4], [5], surface roughness [6]–[10], porous surface [11], [12], structured surface such as microchannel [13]–[16]. The bubble diameter, bubble frequency, wetted surface area and surface wettability influence the critical heat flux as well as heat transfer coefficient. Zupancic et al. [17] studied the PBHT enhancement through hydrophobic plain surface developed by polydimethylsiloxane-silica coating. Jo et al. [19] employed hydrophobic dots on the hydrophilic substrate to improve the critical heat flux (CHF) and nucleate boiling. Betz et al. [20] investigated the PBHT from hydrophilic and hydrophobic patterns employed on the smooth and flat surfaces to improve pool boiling heat transfer. It was found that CHF and HTC for hydrophilic surface (wetting angle=7°) increased up to 65% and 100%, respectively. Jo et al. [21] investigated the PBHT from heterogeneous wettability surface composed of hydrophobic dots on a hydrophilic plain surface. They reported that heterogeneous surface wettability composed of hydrophobic dots on a hydrophilic surface provides better nucleate boiling heat transfer than a homogeneous wettability surface (hydrophilic or hydrophobic). Bourdon et al. [22] studied the effect of wettability on the onset of boiling on the nanometrically smooth surface. Clegg et al. [23] presented the facile, scalable and tuned bulk micro-manufacturing approach for altering the surface topology of copper at the micro- and nano-length scales which significantly influenced the wetting characteristics. Extreme wetting characteristic, contact angle of zero, was obtained by tuning the bulk micro-manufacturing process. Lee et al. [24] demonstrated copper (Cu)-assisted chemical etching process to obtain hierarchically rough silicon surfaces. Thereafter it was modified by spin-coating of a thin layer of Teflon precursor with low surface energy to obtain superhydrophobic surface. The literature presented above suggests the various methods of preparation of hydrophilic and hydrophobic surface. The significant influence of surface wettability on PBHT is also presented. Few complex techniques of the preparation of biphilic surface are also recommended in the literature. However, most of the studies were carried out on plain and smooth surface. In their previous study [18], authors observed improvement in PBHT by using stepped microchannel. In the present investigation, the stepped microchannel is made biphilic by converting the channel hydrophilic by chemical etching and channel top hydrophobic, by surface roughness method.

2. Sample Preparation

The square microchannel (SM-1.0) and stepped (SM-1.6) microchannel are fabricated, as shown in Fig. 1 (A), on the smooth circular face of the 20 mm diameter and 20 mm length copper sample by Vertical Machining Centers (VMC) machining. Thereafter sample is rigorously cleaned in acetone and distilled water. Fig. 1 (B) illustrates the dimension of the stepped microchannel which is verified by the SEM measurement. In addition to that, Fig. 1 (B) shows the fin top region and the stepped microchannel region. The non-reactive mask is applied as shown in Fig.1 (C) on the fin top to avoid the direct contact of the chemical solution during the etching process. The copper is etched by the agent group called as metallographic etching agent as recommended by [23]. The solution of 3:3:2 by volume of ethanol (99.5%), deionized water, and hydrogen peroxide (30 wt.% in water) is prepared. The sample is immersed in the prepared solution thereafter and kept in an oven at 98°C for 120 mins. High temperature environment is maintained to stimulate the redox reaction. The sample is allowed to pass through cooling in the oven for next 180 mins. The fin top is polished by 50 strokes of 1200 grit sandpaper after removal of the mask. Thus, variable surface wetting characteristics as well as variable nucleation site densities are obtained on stepped microchannel. Fig.1 (D) and Fig.1 (E) illustrate the hydrophobic, mirror finished fin top and the hydrophilic channel region, respectively.

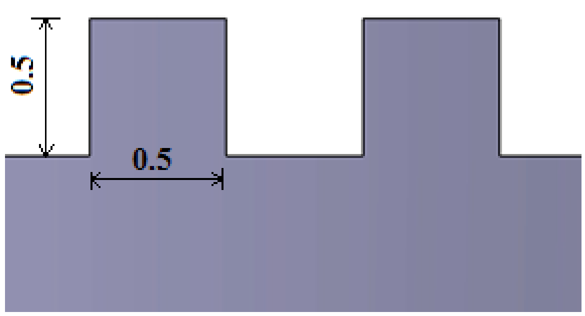

(A)

Machining of 20 mm diameter and 20 mm length sample by VMC to get square microchannel (SM-1.0)

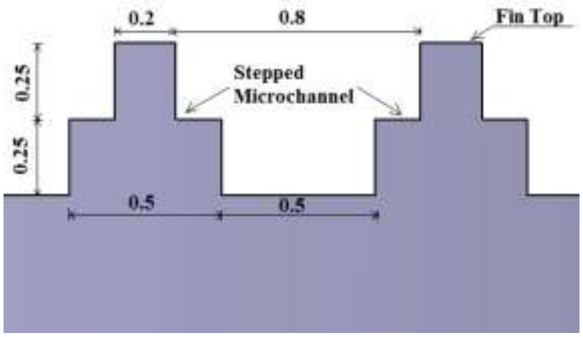

(B)

Machining of the sample by VMC to get stepped microchannel (SM-1.6)

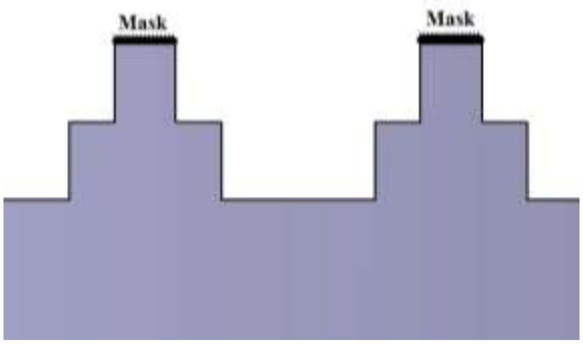

(C)

Non-reactive mask is applied on the fin top before etching process.

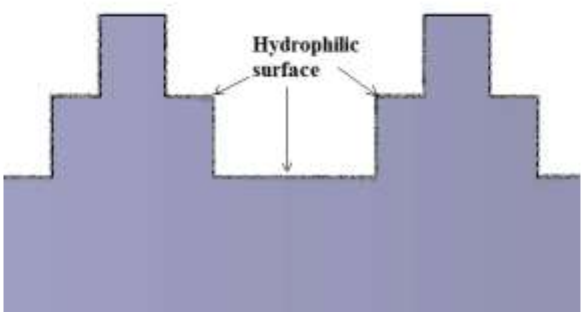

(D)

Hydrophilic surface obtained after Thermo-catalytic etching

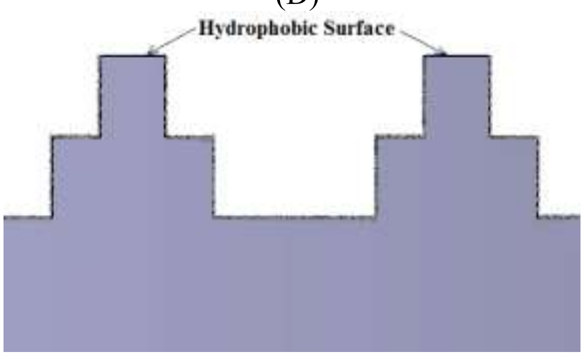

(E)

Hydrophobic surface is obtained by mechanical polishing

Fig. 1 Sample Preparation

3. Experimentation

The experimentation is carried on the experimental setup shown in Fig. 2 which primarily comprises of a chamber with test section assembly and condenser section. The chamber has flanges at its bottom as well as on the top. The top flange is fixed with the condenser assembly. The bottom flange provides the housing to the test section assembly. The boiling chamber provides external fittings to *K*-type thermocouple and pressure transducer at its side plates to record the fluid temperature and operating pressure, respectively. The auxiliary heaters of 2000 W capacity are also fixed at the side plates of the boiling chamber. These heaters maintain the distilled water at saturated condition. The side plates also have watch windows of toughened borosilicate glass having diameter of 115 mm and thickness of 15 mm. These windows helps to visualize the boiling over the test surface. The high-speed camera of 1000 fps is used to conduct the visualization study. It is very essential to maintain the constant pressure inside the boiling chamber which is done by integration of pressure transducer, PID controller and water pump. PID controls the water pump so as to regulate the water supply through the condenser coil. Pressure Relief Valve (PRV) is also installed to safeguard the boiling chamber from the overpressure event. The data acquisition system of cDaq-9178 with NI-9213 is used to obtain and record the temperature readings.

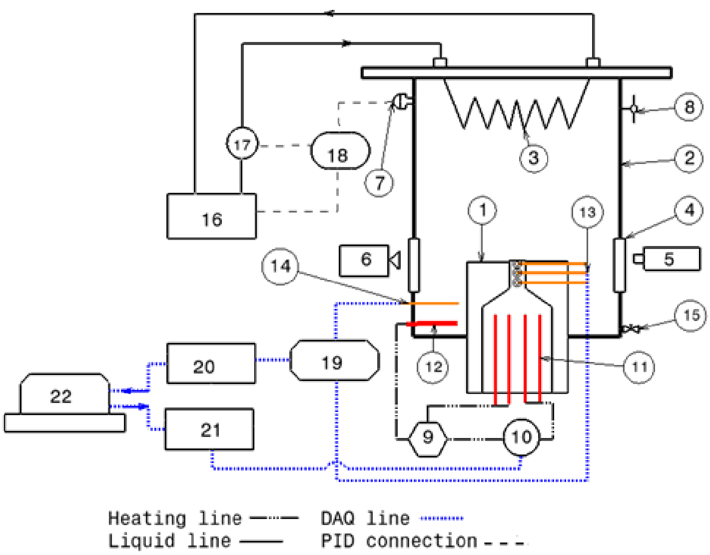

1	Test Section
2	Boiling chamber
3	Condenser coil
4	Sight glass
5	CCD camera
6	Light source
7	Pressure sensor
8	PRV
9	Mains supply
10	Programmable Power supply
11	Main cartridge heater
12	Auxiliary heater
13	Test section thermocouple
14	Bulk fluid thermocouple
15	Drain
16	Water tank
17	Pump
18	PID
19	NI 9213
20	cDaq-9178
21	NI 9264
22	Workstation

Fig. 2 Experimental setup

4. Test Section

The test section assembly comprises of cartridge heater, heating block, test piece and Teflon block is shown in **Fig. 3**. The copper block is hollow at its bottom so as to accommodate the cartridge heater (1500 W) into it. The threads are made on the top of the copper block so as to attach test sample. A thin coat of thermal paste is applied on the heating block so as to ensure the air tight fitting. This assembly is perfectly insulated with a layer of glass wool and the Teflon block. The *K*-type thermocouples are inserted in the sample through 1 mm diameter hole at a spacing of 4 mm (Δx). The first thermocouple is located at 2 mm below the boiling surface (x_{m-1}) and thus, three thermocouples are used to measure the temperature. An incremental heat is given to the test sample and once the steady-state reaches, the temperature readings are recorded and the heat dissipate to the water can be calculated by **Equation 1**.

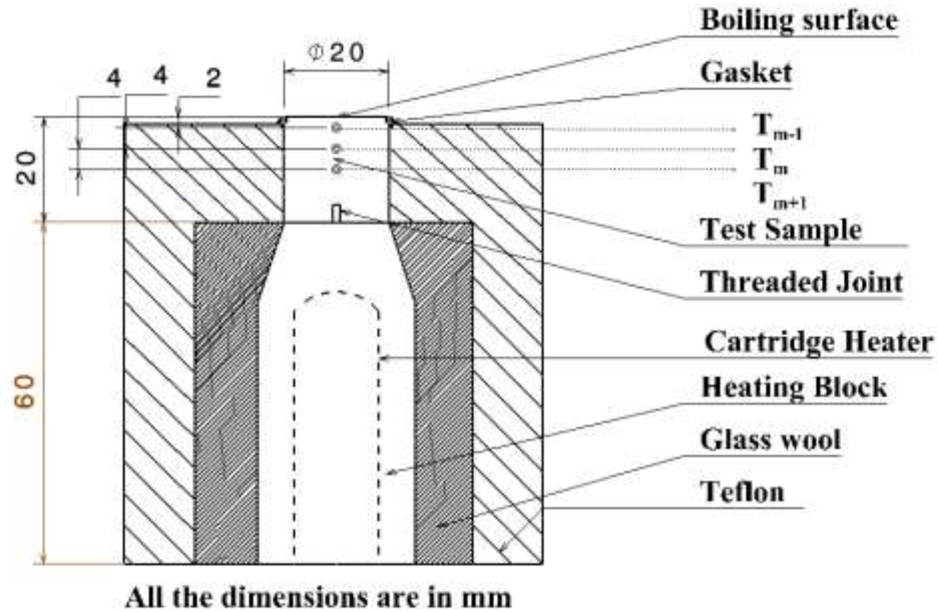

Fig. 3 Test Section

$$q'' = -k_{Cu} \frac{T_{m-1} - T_{m+1}}{2\Delta x} \quad (1)$$

The temperature of the boiling surface is estimated by using **Equation (2).**

$$T_s = T_{m-1} - q'' \left(\frac{x_{m-1}}{k_{Cu}}\right) \quad (2)$$

Heat transfer coefficient (HTC) for water is estimated by **Equation (3).**

$$h = \frac{q''}{(T_s - T_f)} \quad (3)$$

5. Result and Discussion

Contact angle measurement is conducted on plain copper surface. The first copper sample is etched similar to that of the process carried on the channel and second plain copper sample is mirror finished as that of the channel top. Contact angle of the water droplet on etched and mirror finished copper sample surface is 22.5° and 74.02°, respectively. Thus, chemical etching and mirror finishing resulted in the hydrophilic and hydrophobic surface, respectively. The liquid spreadability through the channel is also observed. It is found that liquid spreadability through the etched channel increased by 140%. It also justifies the hydrophilicity of the etched channel.

Fig. 4 represent the boiling curves of the plain surface, untreated SM and biphilic SM. The critical heat flux of plain surface is found to be 877.23 kW/m^2 at wall superheat of 18.18°C. The untreated SM yields CHF of 2028.40 kW/m^2 at wall superheat of 12.25°C. On the other hand, biphilic SM yields CHF of 2592.41 kW/m^2 at wall superheat of 11.50°C. Thus, the sample prepared in the present work enhances CHF by 195.52% as compared to plain surface whereas the CHF of the biphilic SM found to be 27.80% higher than that of untreated SM. **Fig. 5** represent the variation in HTC with the heat flux of plain surface, untreated SM and biphilic SM. The plain surface and untreated SM yield the HTC of 48.25 kW/m^2K and 165.58 kW/m^2K at CHF. The biphilic SM on the other hand yields the HTC of 225.33 kW/m^2K at corresponding CHF. The HTC for untreated SM has increased by 243.17% compared to plain surface. The present study of the development of biphilic SM yields 36.08% higher HTC compared to the untreated SM.

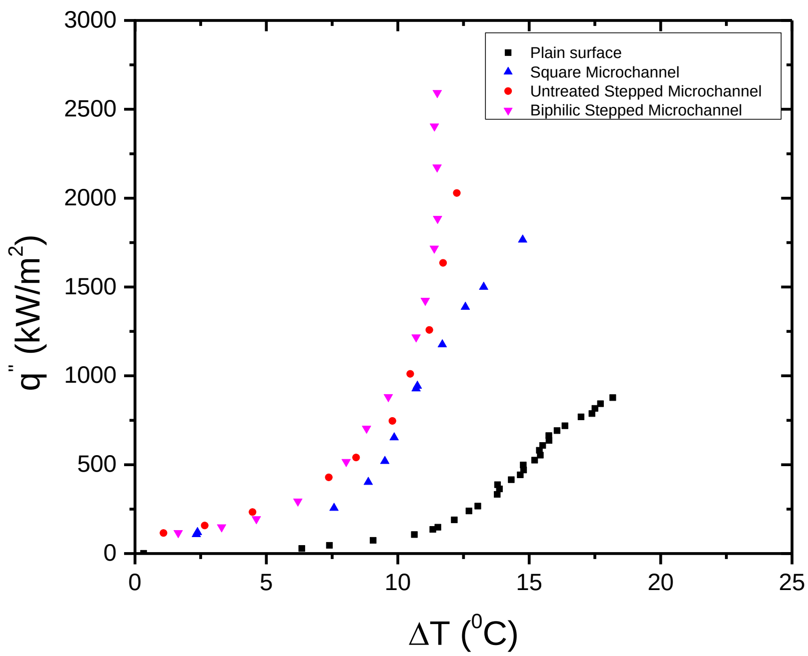

Fig. 4 Boiling curves of plain and different microchannel

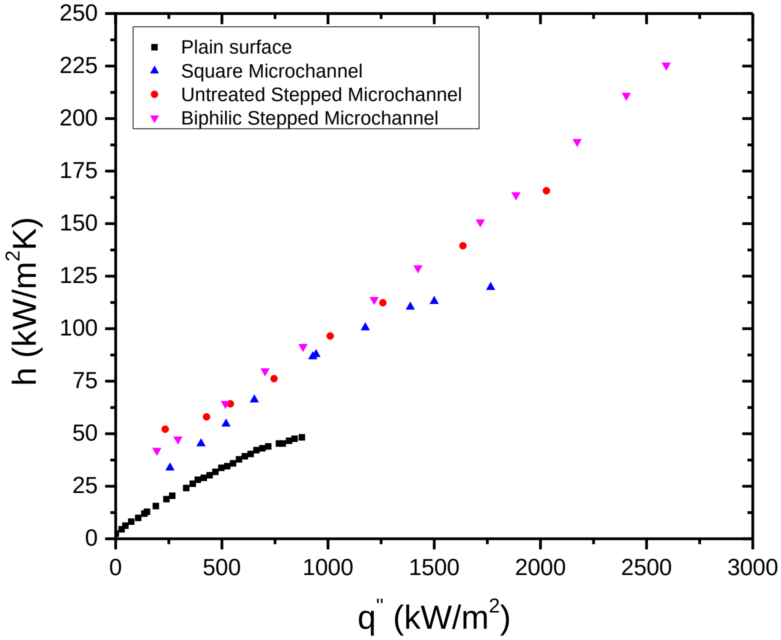

Fig. 5 Heat Transfer coefficient of tested samples at different heat flux

Fig. 6 is the schematic view of the nucleated bubble and the pattern of liquid supply. Compared to the square microchannel, the unique feature of the stepped microchannel is to provide increased number of nucleation site density [18]. The bubble forms at the corner of the stepped channel. Hydrophilic surface offers increased surface wetting characteristics. The improved surface wetting provides the continuous liquid supply to the nucleation sites in the channel. The dry-out area formed at the base of the bubble can be replenished by the surrounding liquid. Quick liquid replenishment is done in the hydrophilic surface after the bubble departure. The bubble nucleated at the corner acquires bilateral as well as transverse liquid supply. Bubble meniscus gets retract from the hydrophilic vertical wall of the channel. Thus, bubble grows vertically upward without negative influence of the channel wall forces. Liquid refilling is also achieved from the fin top through the hydrophilic wall.

Fig. 7 is the schematic view of the bubble growth and coalescence. The hydrophobic surface present between two hydrophilic channels play vital role to govern the bubble departure and bubble coalescence. Nucleation sites disappears as surface is polished to become mirror finished and thus, bubble does not nucleate at the fin top. Bubble nucleated at the channel corner grows over the channel height at high heat flux. During the vertical bubble growth, bubble get repelled from the channel top. Bubbles in the adjacent channel do not get merge where fin top remains flooded. Thus quick liquid supply is ensured even at high heat flux which retard the formation of vapor blanket over the surface.

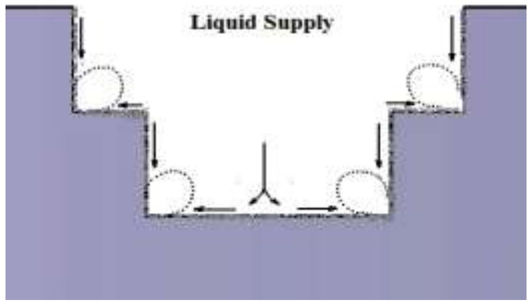

Fig. 6 Pattern of liquid supply

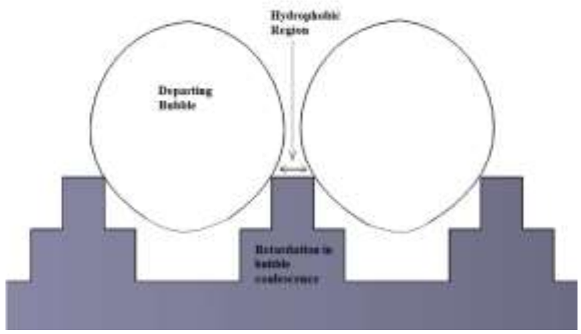

Fig. 7 Mechanism of bubble growth

6. Conclusion

The chemical etching of the channel region has increased the liquid spreadability by 140%. The hydrophobic mirror finished fin top region between two channel regions avoids the lateral bubble coalescence. The liquid flow takes place from the channel top to the channel bottom at high heat flux due to uncovered fin top. This aspect of the pool boiling enhances the critical heat flux by 195.52%.

Liquid spreadability through the channel remarkably increased which assures the quick liquid replenishment to the dry-out area on the bubble departure. Dry-out area at the base of the bubble refills to form next bubble cycle. This feature enhances the heat transfer coefficient by 367.00%.

References

[1] Z. G. Xu and C. Y. Zhao, “Influences of nanoparticles on pool boiling heat transfer in porous metals,” *Appl. Therm. Eng.*, vol. 65, no. 1–2, pp. 34–41, 2014.

[2] C. Leng, X. D. Wang, and T. H. Wang, “An improved design of double-layered microchannel heat sink with truncated top channels,” *Appl. Therm. Eng.*, vol. 79, pp. 54–62, 2015.

[3] S. H. Bhavnani, G. Fournelle, and R. C. Jaeger, “Immersion-cooled heat sinks for electronics: Insight from high-speed photography,” *IEEE Trans. Components Packag. Technol.*, vol. 24, no. 2, pp. 166–176, 2001.

[4] H. Yeom, K. Sridharan, and M. L. Corradini, “Bubble Dynamics in Pool Boiling on Nanoparticle-Coated Surfaces,” *Heat Transf. Eng.*, vol. 36, no. 12, pp. 1013–1027, 2015.

[5] B. J. Zhang, J. Park, and K. J. Kim, “Augmented boiling heat transfer on the wetting-modified three dimensionally-interconnected alumina nano porous surfaces in aqueous polymeric surfactants,” *Int. J. Heat Mass Transf.*, vol. 63, 2013.

[6] J. P. Mchale, “Nucleate boiling from smooth and rough surfaces - Part 1 : Fabrication and

characterization of an optically transparent heater-sensor substrate with controlled surface roughness.” 2013.

[7] L.-W. Fan, J.-Q. Li, L. Zhang, Z.-T. Yu, and K.-F. Cen, “Pool boiling heat transfer on a nanoscale roughness-enhanced superhydrophilic surface for accelerated quenching in water,” *Appl. Therm. Eng.*, vol. 109, pp. 630–639, 2016.

[8] J. M. S. Jabardo, G. Ribatski, and E. Stelute, “Roughness and surface material effects on nucleate boiling heat transfer from cylindrical surfaces to refrigerants R-134a and R-123,” *Exp. Therm. Fluid Sci.*, vol. 33, no. 4, pp. 579–590, 2009.

[9] A. Walunj and A. Sathyabhama, “Transient CHF enhancement in high pressure pool boiling on rough surface,” *Chem. Eng. Process. - Process Intensif.*, vol. 127, no. March, pp. 145–158, 2018.

[10] A. Walunj and A. Sathyabhama, “Bubble Dynamics and Enhanced Heat Transfer During High-Pressure Pool Boiling on Rough Surface,” *J. Thermophys. Heat Transf.*, pp. 1–13, 2018.

[11] C. Young Lee, M. M. Hossain Bhuiya, and K. J. Kim, “Pool boiling heat transfer with nano-porous surface,” *Int. J. Heat Mass Transf.*, vol. 53, no. 19–20, pp. 4274–4279, 2010.

[12] R. Furberg and B. Palm, “Boiling heat transfer on a dendritic and micro-porous surface in R134a and FC-72,” *Appl. Therm. Eng.*, vol. 31, no. 16, 2011.

[13] A. Sitar and I. Golobic, “Effect of Nucleation Cavities on Enhanced Boiling Heat Transfer in Microchannels,” *Nanoscale Microscale Thermophys. Eng.*, vol. 20, no. 1, pp. 33–50, 2016.

[14] A. Jaikumar and S. G. Kandlikar, “Enhanced pool boiling heat transfer mechanisms for selectively sintered open microchannels,” *Int. J. Heat Mass Transf.*, vol. 88, pp. 652–661, 2015.

[15] D. Cooke and S. G. Kandlikar, “Effect of open microchannel geometry on pool boiling enhancement,” *Int. J. Heat Mass Transf.*, vol. 55, no. 4, pp. 1004–1013, 2012.

[16] C. M. Patil and S. G. Kandlikar, “Pool boiling enhancement through microporous coatings selectively electrodeposited on fin tops of open microchannels,” *Int. J. Heat Mass Transf.*, vol. 79, pp. 816–828, 2014.

[17] M. Zupančič, M. Steinbücher, P. Gregorčič, and I. Golobič, “Enhanced pool-boiling heat transfer on laser-made hydrophobic/superhydrophilic polydimethylsiloxane-silica patterned surfaces,” *Appl. Therm. Eng.*, vol. 91, 2015.

[18] A. Walunj and A. Sathyabhama, “Comparative study of pool boiling heat transfer from various microchannel geometries,” *Appl. Therm. Eng.*, vol. 128, 2018.

[19] H. J. Jo, S. H. Kim, H. S. Park, and M. H. Kim, “Critical heat flux and nucleate boiling on several heterogeneous wetting surfaces: Controlled hydrophobic patterns on a hydrophilic substrate,” *Int. J. Multiph. Flow*, vol. 62, pp. 101–109, 2014.

[20] A. R. Betz, J. Xu, H. Qiu, and D. Attinger, “Do surfaces with mixed hydrophilic and hydrophobic areas enhance pool boiling?,” *Appl. Phys. Lett.*, vol. 97, no. 14, pp. 2012–2015, 2010.

[21] H. Jo, H. S. Ahn, S. Kang, and M. H. Kim, “A study of nucleate boiling heat transfer on hydrophilic, hydrophobic and heterogeneous wetting surfaces,” *Int. J. Heat Mass Transf.*, vol. 54, no. 25–26, pp. 5643–5652, 2011.

[22] B. Bourdon, E. Bertrand, P. Di Marco, M. Marengo, R. Rioboo, and J. De Coninck, “Wettability influence on the onset temperature of pool boiling: Experimental evidence onto ultra-smooth surfaces,” *Adv. Colloid Interface Sci.*, vol. 221, pp. 34–40, 2015.

[23] N. Clegg, K. Kota, X. He, and S. Ross, “Achieving Ultra-Omniphilic Wettability on Copper Using a Facile, Scalable, Tuned Bulk Micromanufacturing Approach,” *J. Micro Nano-Manufacturing*, vol. 5, no. 3, p. 031003, 2017.

[24] J. P. Lee, S. Choi, and S. Park, “Extremely superhydrophobic surfaces with micro- and nanostructures fabricated by copper catalytic etching,” *Langmuir*, vol. 27, no. 2, pp. 809–814, 2011.

Contribution of Individual Authors to the Creation of a Scientific Article (Ghostwriting Policy)

The authors equally contributed in the present research, at all stages from the formulation of the problem to the final findings and solution.

Sources of Funding for Research Presented in a Scientific Article or Scientific Article Itself

No funding was received for conducting this study.

Conflict of Interest

The authors have no conflicts of interest to declare that are relevant to the content of this article.